JOURNAL OF CATALYSIS 87, 36–54 (1984)

Investigation of Supported Iron Fischer–Tropsch Synthesis Catalysts by Mössbauer Spectroscopy

L. M. TAU, S. BORCAR, D. BIANCHI, AND C. O. BENNETT

Department of Chemical Engineering, University of Connecticut, Storrs, Connecticut 06268

Received April 7, 1983; revised December 8, 1983

The carburization of the iron in a 10% Fe on Al_2O_3 (Alon-C) catalyst has been followed by Mössbauer spectroscopy. The studies were made mostly at 270–285°C and the catalyst was exposed to CO/H_2 and CO/He gas mixtures. The decarburization by H_2 was also studied. The principal carbides found are χ-carbide, $Fe_{2.5}C$, ε'-carbide, $Fe_{2.2}C$ with a tendency for a preponderance of the latter at long reaction times. The carburization by CO is promoted by the presence of H_2, even in a small concentration. The promoting action of H_2 seems to be related to the ease of carburizing a particle with a well-reduced surface. Adding water to CO/H_2 slows the carburization rate without slowing the carbon deposition rate. Similar experiments with 10% Fe/SiO_2 (Cab-O-Sil) catalyst give similar results. Rates are somewhat reduced, but there is no qualitative change introduced by the different support.

INTRODUCTION

In a previous study (*1*) we have reported on the evolution of the bulk and surface compositions of a reduced 10% Fe/Al_2O_3 catalyst as it is exposed to 10% CO/H_2 at 1 atm and 285°C. In further work (*2*) we have given more evidence on the nature of the species observed as the state of the catalyst changes with reaction times between 0 and 2 or 3 h. The degree of carburization of the bulk has been measured by Mössbauer effect spectroscopy (MES), but the discussion of the progression of the bulk composition was limited to that necessary to account for the carbon deposited during the reaction (*1, 2*). In the present paper we give more details of the MES work. In particular we present the evolution of the spectra during reaction (carburization) and attempt to identify the various kinds of carbides observed. We also present MES results obtained during decarburization in H_2 and during several other treatments.

Before concentrating on the MES work, it is useful to consider the sequence of events proposed in our previous work (*1, 2*). As a freshly reduced Fe/Al_2O_3 catalyst is exposed to 10% CO/H_2 at 285°C, there is an initial burst of methane production, and after a few minutes an approximately constant product distribution is obtained, similar to that reported by Vannice (*3*). After a few seconds, the methane production rate goes through a minimum, and then after about 10–15 min, all the hydrocarbon rates go through a broad maximum, after which the rates fall gradually until the end of the 2–3 h experiments. A switch to H_2 at various points during the reaction leads to peaks, almost entirely of methane, made from the hydrogenation of the various surface- and bulk-carbon-containing species (*1, 2*). There seems to be a limited amount of surface CH which is the active precursor of methane and higher products. In addition, there is a surface carbide which builds up to a maximum quantity at about the time of the maximum reaction rate. There is also some inert graphitic carbon which appears at longer times, as the catalyst deactivates. Finally, there are various bulk carbides, which accumulate during reaction, and these are the principal subject of this paper.

An extensive MES study of mostly bulk iron catalysts has been presented by Niemantsverdriet *et al.* (*4–6*). Silica-supported iron catalysts have been investi-

0021-9517/84 $3.00

gated by Raupp and Delgass (*7–9*) and by the group at Northwestern (*10–14*). Carbon-supported iron has been studied by MES and other techniques by Jung *et al.* (*15*), and alumina-supported iron by Nahon (*16*). We shall compare our work with some of the foregoing studies, but the effects of differences in the iron environment and in the reaction temperature and CO/H_2 feed ratio are not well known. The present MES work was done in an *in situ* cell (*17*) arranged so that the catalyst was exposed to the same conditions as were used in our previous studies (*1, 2*). Thus we can make useful correlations between the MES results and these previous kinetic studies.

As with most spectroscopies, the study of mixed phases by MES is most reliable when spectra are available of the pure phases. For the iron carbides the spectra of cementite (θ-Fe_3C), Hagg carbide (χ-$Fe_{2.5}C$), and Fe_7C_3 ($Fe_{2.33}C$) are well established and are a familiar field of study for metallurgists (*18, 19*). However, the metastable carbides such as ε'-$Fe_{2.2}C$ are apparently found only in iron carburized during the Fischer–Tropsch reaction, typically at 250–300°C. What is more, they have not yet been prepared as pure phases. Thus, there are some difficulties in interpreting the MES results for mixed carbides (*5, 18*).

We shall follow the nomenclature of Niemantsverdriet *et al.* (*5*). We observe that as Fe/Al_2O_3 is progressively carburized at 285°C in 10% CO/H_2. Fe_xC, χ-$Fe_{2.5}C$, and ε'-$Fe_{2.2}C$ are formed with the nomenclature of Niemantsverdriet (*4, 5*). The evolution of composition is not inconsistent with the usual order of stability of the carbides. As the ε' form is heated it looses carbon as the χ-form and then the θ-form are favored.

Before passing to the experimental findings, a final general comment is pertinent. By MES we find that the proportions of the various carbides change during carburization and decarburization. This is a strong argument in favor of the generally accepted idea that the rate of carburization is controlled by the reaction of dissolved carbon and iron, in highly divided supported iron. If the rates were controlled by the diffusion of dissolved carbon, the proportion of the various carbides formed by a relatively rapid chemical equilibration behind an advancing diffusion front should remain constant. For the 160–190 Å iron particles of the present work, any reasonable value of the diffusivity of carbon would lead to complete carburization in a time of less than a second, if diffusion were the rate-limiting step. Measured times are of the order of an hour.

EXPERIMENTAL METHODS

Catalyst preparation. The catalysts were prepared on two different support materials: (A) Alumina; Alon-C, P-110 from Degussa, area 100 m^2/g, pore size 200 Å; and (B) Silica: Cab-O-Sil 1, M5 from Cabot, area 250 m^2/g. The metal loading for each case was 10 wt%. The alumina-supported catalyst was prepared by the precipitation technique of Nahon *et al.* (*16*) and is the same as that used in the studies by mass spectrometry (*1, 2*). The silica-supported catalyst was prepared by the impregnation of Cab-O-Sil with an aqueous solution of $Fe(NO_3)_3 \cdot 9H_2O$ by the incipient wetness method. The catalyst was dried at 120°C for 24 h in air. About 250 mg of the supported catalyst, pressed into a 16-mm-diameter self-supporting pellet, served as the TMES sample. The effective thickness is 5.27.

Mössbauer instrumentation. Transmission spectra were obtained in the constant-acceleration mode with an Elscinct Mössbauer spectrometer with a Model MFG 3A function generator, MVT-3 linear velocity transducer, and a MD-3 transducer driving unit. A Reuter–Stokes $Kr–CH_4$ proportional counter, powered by an Ortec 401A modular system bin/456 high-voltage power supply, was used for γ-ray counting. Voltage pulses from the detector were amplified by an Ortec 142 PC preamplifier and an Ortec 571 spectroscopy amplifier module. The entire system was coupled with a Tracor

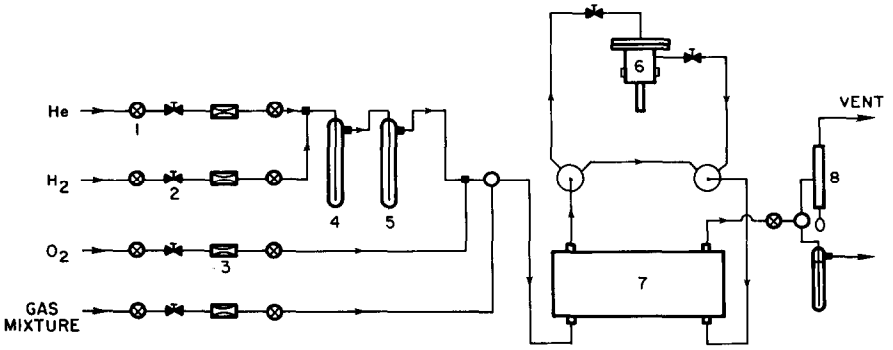

FIG. 1. Flow system for the Mössbauer experiments. (1) On–off valve; (2) Needle valve; (3) Venturi flowmeter; (4) Deoxo unit; (5) Liquid-nitrogen trap; (6) Mössbauer cell; (7) Thermal conductivity (TC) cell; (8) Bubble meter.

Northern Model NS-710A multichannel analyzer (MCA), and data from the MCA were dumped onto a paper tape using an ASR-33 teletypewriter. The setup was capable of counting 100,000 counts/h per channel.

The 14.414 KeV Mössbauer radiation was obtained from a 85 mCi ^{57}Co/Pd source (New England Nuclear). The hyperfine spectrum of a 12.5-μm Fe foil was used to provide a linearity check, and to define a zero for isomer shift calculations. The outer lines of the six-peak Fe^0 spectrum (linewidth 0.264 mm/s) were used for velocity calibrations.

Treatment system. A stainless-steel Mössbauer transmission cell with beryllium windows was used for "*in situ*" catalyst reaction and treatment (*17*). Heating was accomplished by using 4 cartridge heaters capable of heating the catalyst sample to 500°C at a rate of 1°C/s. Temperature control for isothermal cell operation was achieved to ±1°C by a Thermoelectric 400 temperature controller capable of operating in the range 0–600°C. A copper jacket skirted the cell, and air circulation in the jacket was used to cool the windows and to cool the cell after temperature treatments. A controlled gas environment (1 atm) of any desired gas mixture could be maintained inside the cell at isothermal conditions for controlled time periods. After treatment, the Mössbauer spectra were recorded at room temperature.

The gas purification and monitoring system is shown in Fig. 1. The gas streams were monitored by Venturi flow meters which were calibrated using a bubble meter at the system exit. The gases obtained from Matheson were H_2 (Prep), He (HP), 33% CO/H_2 (HP). Gas mixtures 10% CO/H_2, 10% CO/He, and 10% ethylene/H_2 were prepared in our lab from UHP components. The H_2 and He streams were purified by using Analabs gas driers, a Deoxo trap, and a liquid-N_2 trap downstream.

The reactant and product streams were passed over the resistance arms of a thermal conductivity detector which was a part of a Gowmac Series 550 gas chromatograph. The difference between the reactant and product streams (owing to the catalytic reaction taking place in the MES cell) was determined by the unbalance of the thermal conductivity bridge and was recorded by a Gowmac Model 70-750 recorder. The TC detector could only determine qualitatively the activity of the catalyst during gas treatment. Overall product determination was made in separate experiments using a differential reactor and a mass spectrometer during the transient response studies (*1, 2*).

The treatment scheme implemented was identical in all cases. The following parameters had to be specified: (1) temperature of

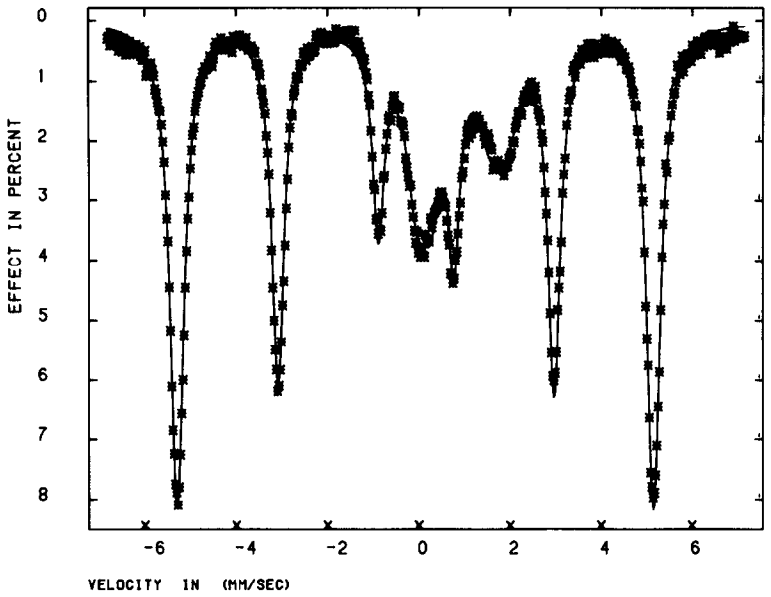

FIG. 2. Mössbauer spectrum of 10% Fe/Al_2O_3 reduced 17 h at 460°C.

treatment (all treatments were isothermal), (2) reactant concentration (10% CO/H_2 etc.), and (3) time of treatment (10 min, etc.). The cell was purged with the reactant stream until the thermal conductivity trace indicated the same input and output streams. The temperature was quickly raised to the desired reaction temperature, and the sample was treated isothermally for the predetermined time of treatment. The cell was then rapidly cooled with blasts of cold air to room temperature. It was found that the rate of reaction was insignificant at $T < 200$°C as determined by the trace of the thermal conductivity detector. Appropriate corrections were made to the time of treatment to account for heating and cooling above 200°C.

The particle size of the final treated catalyst was determined (after H_2 reduction) by X-ray diffraction line-broadening and the Scherrer equation. A Phillipps X-ray diffractometer using Cu$K\alpha$ radiation and a scintillation counter was used in the determination of the diffraction patterns. The following particle sizes were (A) 10% Fe/Alon-C: (i) D = 160 Å, treatment temp $T \leq$ 460°C, (ii) D = 190 Å treatment temp $T >$ 460°C; (B) 10% Fe/Cab-O-Sil: (i) D = 120 Å, treatment temp $T \leq$ 460°C, (ii) D = 190 Å, treatment temp $T \geq$ 460°C. Particle size analyses using Transmission Electron Microscopy (TEM) indicated a range of particle sizes: (A) D = 160–200 Å for the 10% Fe/Alon-C and (B) D = 110–130 Å for 10% Fe/Cab-O-Sil. The reduction temperature was 460°C.

RESULTS

Fe/Alon-C 10%

Identification of carbides. The catalyst disk in the MES cell was reduced as follows. The sample was first heated in helium at 250°C for 2 h to remove as much moisture as possible before reduction (*7*). The treatment gas was then switched to H_2, the sample was heated quickly to 460°C, and reduction was continued for 17 h. The MES result for the catalyst reduced in this manner is shown in Fig. 2 and the Mössbauer parameters are given in Tables 1a and b.

Figure 2 and subsequent spectra have been plotted by computer techniques, based on the program developed by Chrisman and Tumolillo (*20*). Some preliminary

TABLE 1a

Mössbauer Parameters of Fe Species Detected over 10% Fe/Alon C at Room Temperature (298 K). (Isomer Shift Data Reported with Respect to α-Fe)

Treatment	Species	Spectral contribution (area %)	Isomer shift, δ (mm/s)	Quadrupole splitting, ΔE_Q (mm/s)	Hyperfine field, H (kOe)
Catalyst after the reduction sequence (Fig. 5a)	Fe^0	76	0.0	0.0	330
	Fe^{2+} (A)	26	1.12	1.02	0.0
	Fe^{2+} (B)		1.08	0.64	0.0
Catalyst carburized at 390°C (Fig. 5b) χ(I) : χ(II) χ(III) = 2.14 : 2.35 : 1	χ-$Fe_{2.5}C$ (I)	84	0.22	0.11	183
	(II)		0.26	0.14	219
	(III)		0.17	0.08	106
	Fe^{2+} (A)	16			
	Fe^{2+} (B)				
Catalyst carburized at 270°C (Fig. 6) χ(I) : χ(II) χ(III) = 2.52 : 2.77 : 1	χ-Fe_5C_2 (I)	29			
	(II)				
	(III)				
	ε'-$Fe_{2.2}C$	58	0.24	0.11	171
	Fe^{2+} (A)	13			
	Fe^{2+} (B)				

work was done based on the program of Wilson and Swartzendruber (*21*). The computed lines correspond to Lorentzian peaks fitted to the data by least-squares methods. For Figs. 2, 3, and 4 no constraints have been used, so that we can compare our Mössbauer parameters and peak area ratios to values from the literature. In order to get a good fit for the spectra it is necessary to include peaks corresponding to two Fe^{2+} sites (*7*). Thus in Fig. 2 the peak areas for Fe^0 are in the ratios 3.3 : 2.13 : 0.93 : 1 : 1.96 : 3.05, compared to the expected 3 : 2 : 1 : 1 : 2 : 3. The area in the four Fe^{2+}

TABLE 1b

Some Details of the Mössbauer Effect Spectra (without any Constraints in the Curve Fitting)

Sample	Center of the peaks, channel number[a]	Area ratios
Fe^0 (Fig. 5a)	57, 138, 219, 278, 359, 439	3.30, 2.13, 0.93, 1.00, 1.96, 3.05
χ-Fe_5C_2 (I) (Fig. 5b) (II) (III)	151, 190, 240, 271, 320, 363	3.06, 1.97, 1.18, 1.00, 2.07, 3.06
	132, 186, 236, 277, 327, 386	2.96, 1.95, 1.11, 1.00, 1.81, 2.95
	193, 215, 244, 266, 291, 315	3.26, 1.93, 1.00, 0.94, 1.96, 3.28
χ-Fe_5C_2 (I) (Fig. 6) (II) (III)	The same as Fig. 5b	2.99, 1.94, 1.00, 1.04, 1.99, 2.99
		3.07, 2.01, 1.00, 0.96, 2.06, 3.07
		2.85, 2.02, 1.00, 1.14, 1.79, 2.91
ε'-$Fe_{2.2}C$ (Fig. 6)	159, 199, 240, 272, 313, 357	2.79, 1.98, 1.11, 1.00, 1.93, 2.81

[a] Total channels = 512.

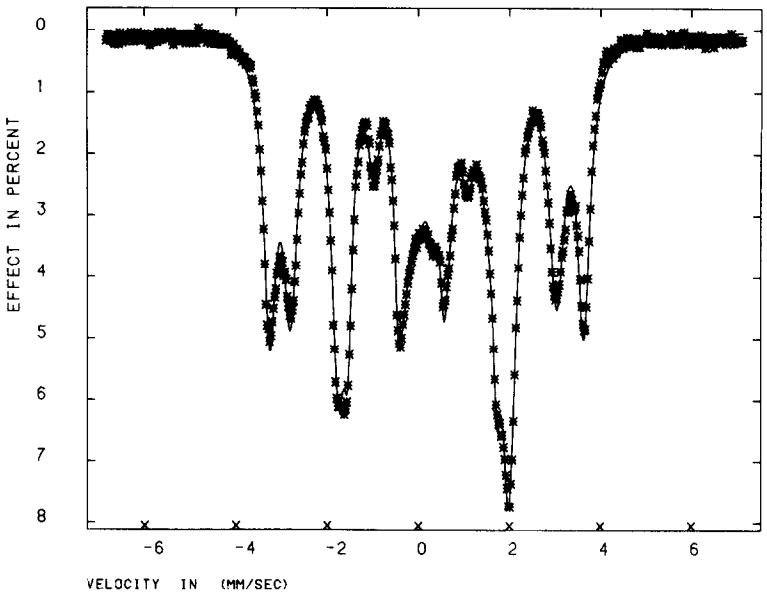

FIG. 3. Mössbauer spectrum of 10% Fe/Al_2O_3 treated in 33% CO/H_2 at 390°C.

peaks in the central part of the spectrum is 26% of the total Fe^0 + Fe^{2+} area.

We have found that the reduced catalyst of Fig. 2 can be converted to a single carbide (χ-form) by extended treatment in 33% CO/H_2 at 390°C, a temperature above that used for the kinetic experiments. The four Fe^{2+} lines persist to the extent of 16%, but the Fe^0, easily detectable by the outer lines, has disappeared. The unconstrained fit to the data of Fig. 3 requires 22 peaks. The Mössbauer parameters for the carbide part of the spectrum are in good agreement with the literature, and the ratios of the iron in the three environments, shown in Tables 1a and b is in reasonable agreement with the expected values; 2:2:1 (*5, 22*). Within each hyperfine field, the ratios are also close to the expected 3:2:1:1:2:3.

For Fig. 3 we were able to prepare the single χ-carbide, but for the metastable ε'-carbide, all treatment conditions led to a mixture of at least the χ- and ε'-carbides, with residual Fe^{2+}. At 270°C, using 10% CO/H_2 for 24 h, a large proportion of ε'-$Fe_{2.2}C$ can be obtained (58% of the total area), and this spectrum is shown in Fig. 4. Although not visible on the scale of Fig. 4, 28 peaks are necessary for a good fit; 6 for ε'-$Fe_{2.2}C$, 18 for χ-$Fe_{2.5}C$, and 4 for Fe^{2+}. The Mössbauer parameters of Tables 1a and b agree with the literature (*4, 10*), and the various area ratios and line positions in this unconstrained fit are reasonable. The ordinate scale on the figures of our previous study (1) which correspond to Figs. 2–4 are not correct. The interpretation is not changed.

Figure 2 is for an uncarburized sample, and Figs. 3 and 4 are for completely carburized samples. The next step in complexity is a partially carburized sample containing the 6 Fe^0 peaks. From now on the fitting procedures will be constrained so that the areas of the 6 peaks of each type of iron in the carbides are in the ratio 3:2:1:1:2:3, as are those for Fe^0. The three kinds of iron in χ-$Fe_{2.5}C$ are constrained to have the area ratios 2:2:1. When this procedure is applied to partially carburized samples (10% H_2/CO at 270 or 285°C for various times) there are still a few small peaks which are not represented by the computer model. Following Niemantsverdriet (*4*), we postulate the existence of an unknown carbide Fe_xC, where $x > 2.5$. The line positions and

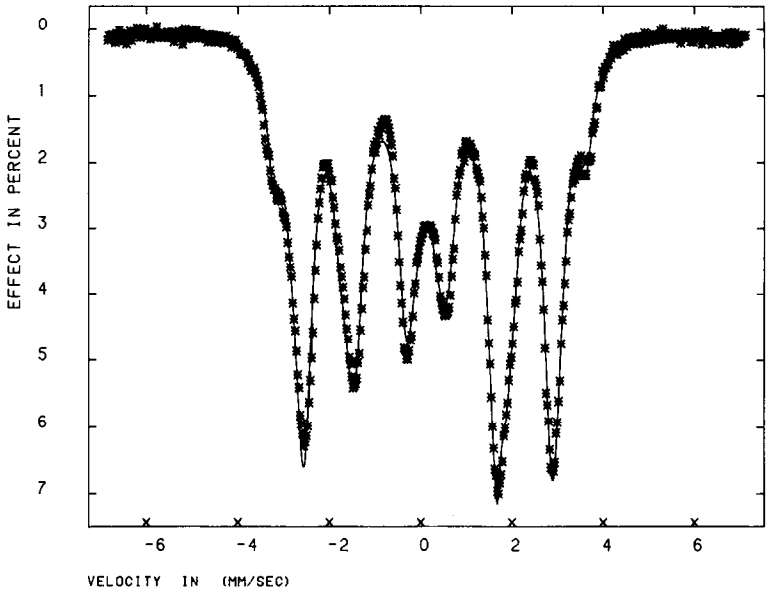

FIG. 4. Mössbauer spectrum of 10% Fe/Al_2O_3 treated in 10% CO/H_2 at 270°C for 24 h.

Mössbauer parameters for Fe_xC are given in Table 2. With this added component it is now possible to analyze the spectra of the partially carburized samples. In general these spectra are now made up of 40 peaks. The parameters for the unknown carbide are similar to those preposed previously (*4, 15*). The line ratios for Fe_xC have been assumed to be in the ratio 3 : 2 : 1 : 1 : 2 : 3. Their inclusion in the fitting of both the visible and hidden peaks in spectra like Fig. 6 improves the fit perceptibly.

TABLE 2

The Mössbauer Parameters of the Unknown Carbide (Fe_xC) and Its Line Positions for 10% Fe/Al_2O_3

Isomer shift,[a] δ (mm/s)	Quadrupole splitting, ΔE (mm/s)	Hyperfine field, H (kOe)
0.18 ± 0.02	0.02 ± 0.02	241 ± 2
Line position[b] (Channel)		
115, 174, 237, 270, 335, 395		

[a] Isomer shift data reported with respect to α-Fe.
[b] The Doppler velocity is 7.0 mm/s, and the total channels are 512.

Carburization and decarburization. One of the principal goals of the present study is to observe the bulk iron composition during transient experiments like those done previously (*1, 2*). At constant temperature (270 or 285°C) the feed flowing to a differential reactor containing reduced catalyst (Fig. 2) is switched from H_2 to 10% CO/H_2. The product composition has been followed by mass spectrometry, and Figs. 5–9 are the MES results obtained during the reaction of 10% CO/H_2 and simultaneous carburization of the iron catalyst. After reacting for 110 min at 270°C, the feed is switched to H_2, and the results shown in Figs. 10–13 are obtained. Table 3 shows the composition of the solid phase deduced from these spectra by the methods already described. As mentioned in the experimental section, the kinetic experiment must be stopped (quenched) at each appropriate time. The acquisition of the MES data then follows, requiring scan times of up to 24 h. An interesting alternative procedure, which involves following one Mössbauer peak, has been used by Raupp and Delgass (*9*).

The results of Table 3 are plotted in Fig 14. The Fe_xC concentration passes through

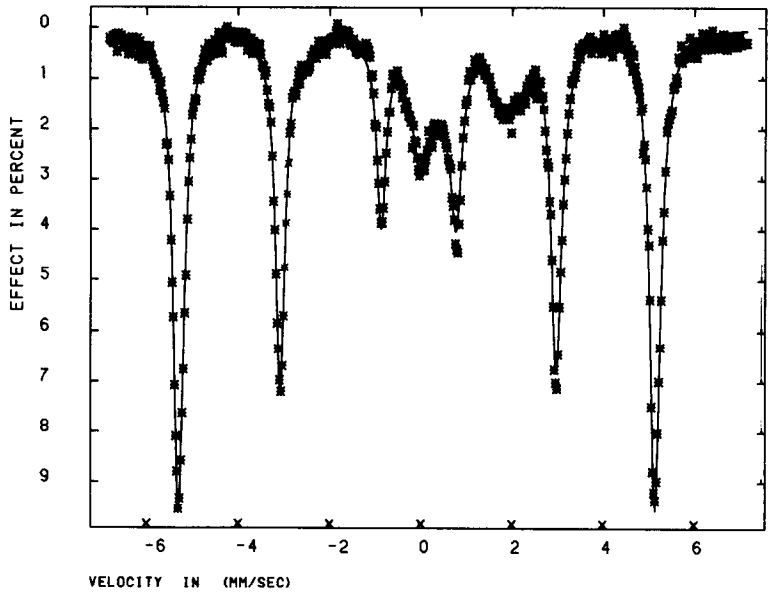

FIG. 5. Mössbauer spectrum of 10% Fe/Al_2O_3 treated in 10% CO/H_2 at 270°C for 6 min.

a maximum during both carburization and decarburization, as does that of χ-$Fe_{2.5}C$. The computer-calculated standard deviations in the area fractions range from 1 to 5%. In Fig. 14 the percentage carbide is calculated with the percentage Fe^{2+} excluded. For example, the percentage total carbide is 100% minus percentage Fe^0.

Effect of gas composition on carburization. Further experiments have been carried out for $H_2 \rightarrow$ 10% $CO/H_2 \rightarrow H_2$ at 285°C (Fig. 15) and for $H_2 \rightarrow$ 33% $CO/H_2 \rightarrow H_2$ at

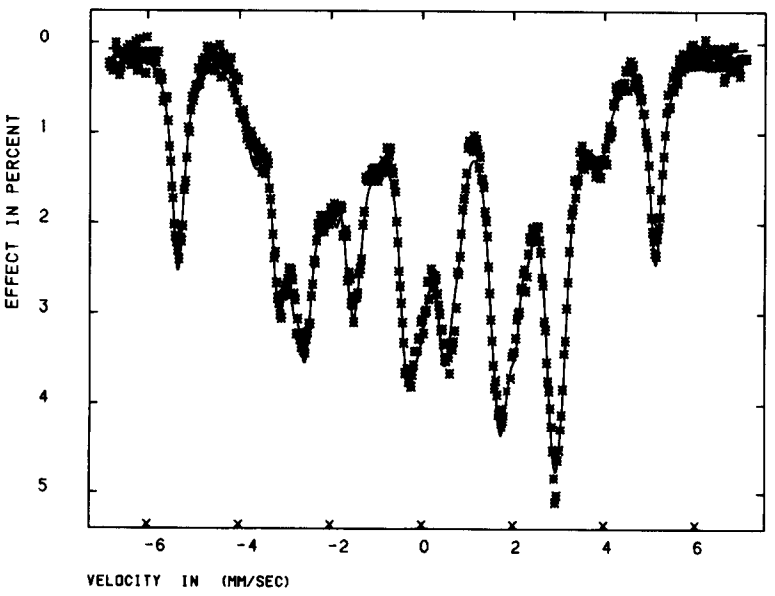

FIG. 6. Mössbauer spectrum of 10% Fe/Al_2O_3 treated in 10% CO/H_2 at 270°C for 22 min.

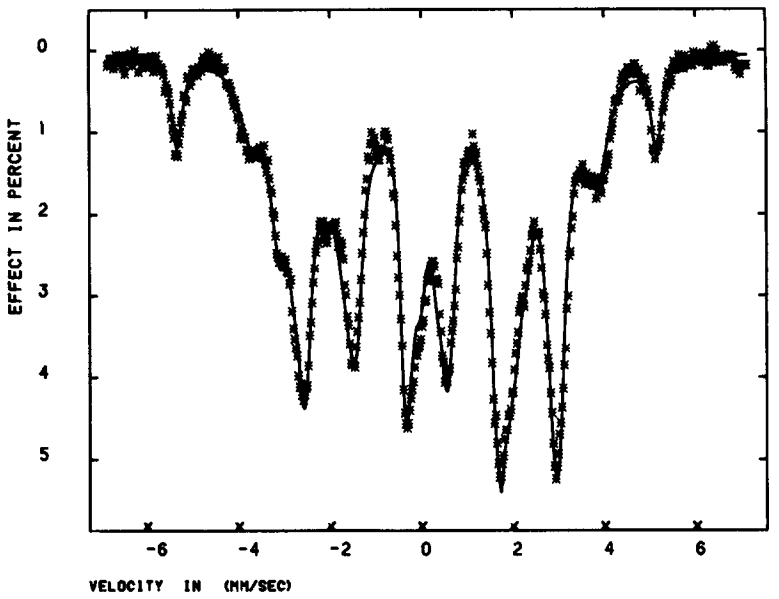

FIG. 7. Mössbauer spectrum of 10% Fe/Al_2O_3 treated in 10% CO/H_2 at 270°C for 46 min.

270°C (Fig. 16). The MES results have been interpreted in the same general way. At higher temperatures and shorter time the χ-form exceeds the ε'-form. The computer fitting of spectra with 40 peaks is tedious and quite expensive, so in Fig. 15 and onward we shall use the constrained fit and not separate out the Fe_xC.

The total carbide results shown in Figs. 14–16 have already been used to interpret the results for the same experimental sequence followed by mass spectrometry (*1*,

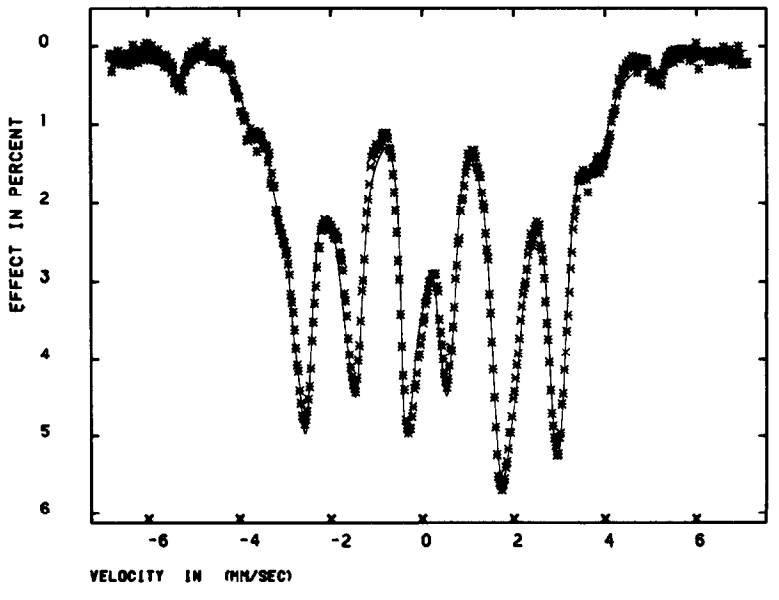

FIG. 8. Mössbauer spectrum of 10% Fe/Al_2O_3 treated in 10% CO/H_2 at 270°C for 77 min.

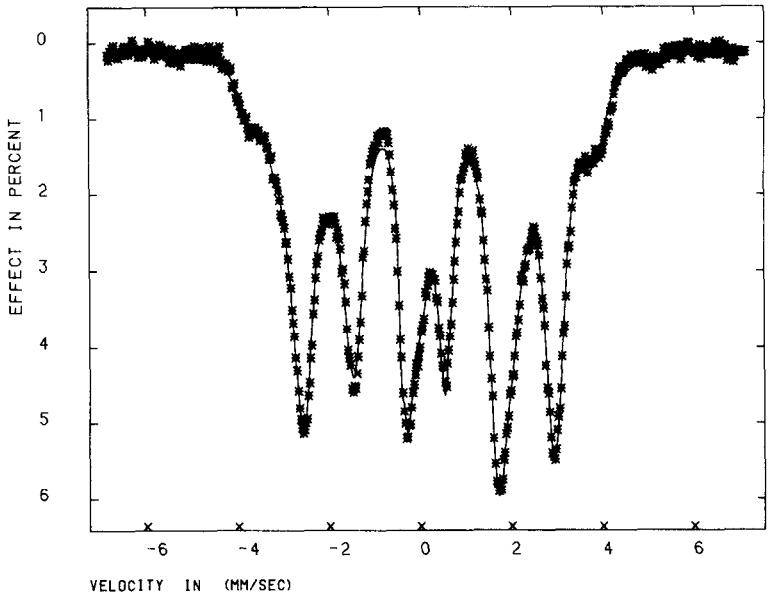

FIG. 9. Mössbauer spectrum of 10% Fe/Al_2O_3 treated in 10% CO/H_2 at 270°C for 110 min.

2). In particular, the methane peak associated with bulk carbide (*1*) agrees with a carbon content which corresponds to a mixture of ε' and χ-carbides. The rate of methane formation is also found to be compatible with the slope of the curves after a switch to H_2. These results support the carbide formulas proposed by Niemantsverdriet (*4*, *5*).

Figure 17 shows the effect of the reaction gas composition on the progress of carburization. An increase in CO in the CO/H_2

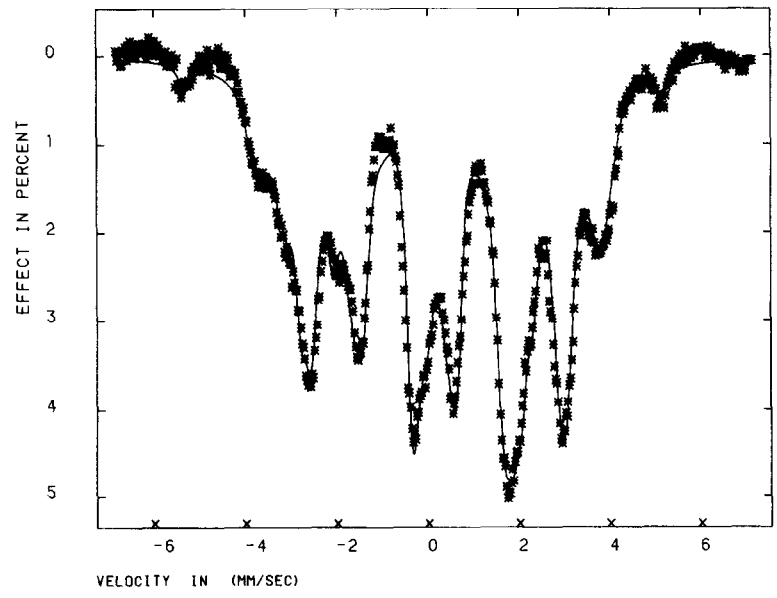

FIG. 10. Sample of Fig. 9 treated in H_2 at 270°C for 18 min.

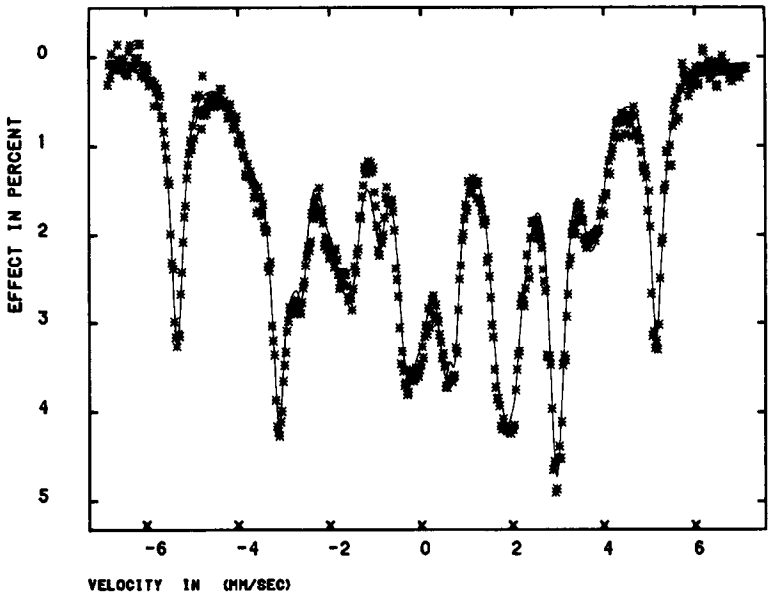

FIG. 11. Sample of Fig. 9 treated in H_2 at 270°C for 29 min.

mixture from 10 to 33% increases the rate of carburization as shown. However, the rate of carbide formation is decreased in the absence of H_2 in the gas, as shown by curve C. A similar result has been discussed by Unmuth *et al.* (*12*). Finally, curve D shows that the addition of water vapor for the 10% CO/H_2 inhibits carburization, and it also inhibits the formation of hydrocarbons (*1*, *13*). The O/H ratio on the surface is higher for curves C and D, and this leads to a lower rate of carburization. However, the

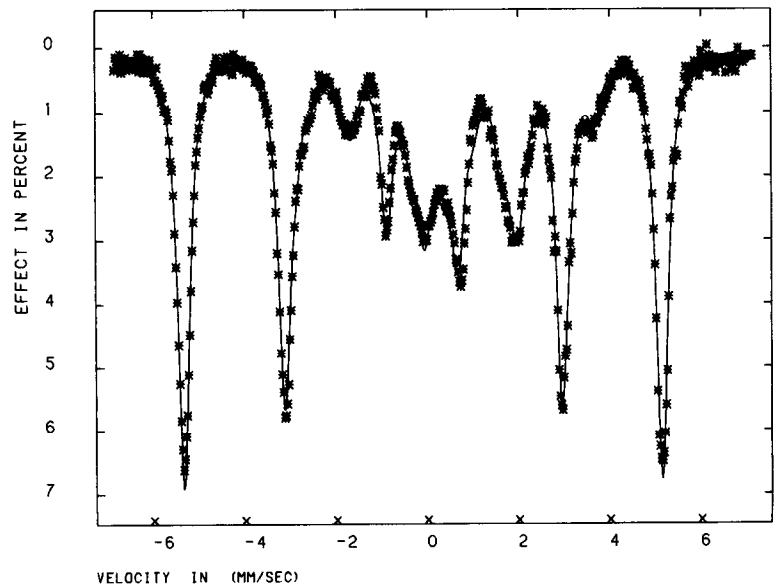

FIG. 12. Sample of Fig. 9 treated in H_2 at 270°C for 45 min.

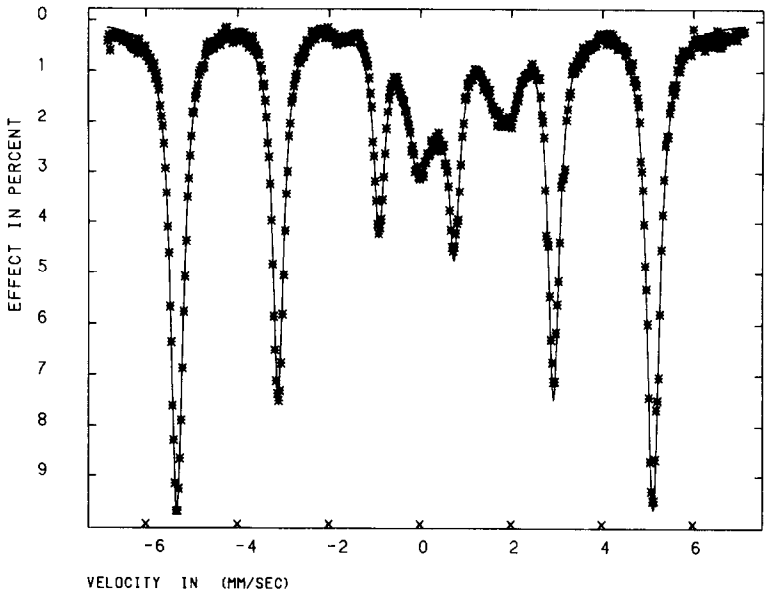

FIG. 13. Sample of Fig. 9 treated in H_2 at 270°C for 69 min.

rate of accumulation of surface carbonaceous species is at least as rapid in these cases (*1, 2*). Thus it is clear that the state of the surface somehow influences the transfer of carbon into solution in the iron crystallites, after which it diffuses and reacts rapidly. It is interesting that this situation seems to be altered at higher temperatures, where χ-$Fe_{2.5}C$ is the predominant carbide. Figure 18 shows the effect of temperature on the rate of total carbide formation in 10% CO/H_2 at various temperatures. At 390°C, we find that the rate of carburization in 10% CO/He (not shown in Fig. 18) is about the same as that in 10% CO/H_2. It would now seem that the O/H ratio on the surface is not so important as it was at 270°C (Fig. 17). In other words, at higher temperatures the rate of carburization is influenced more by the bulk reaction of iron

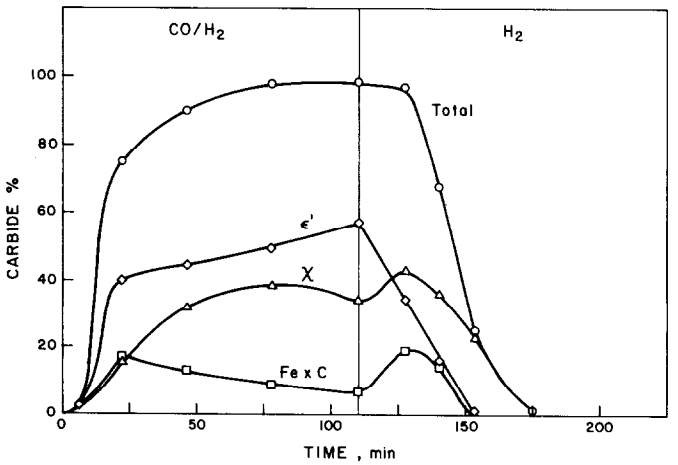

FIG. 14. Freshly reduced 10% Fe/Al_2O_3 carburized in 10% CO/H_2 and decarburized in H_2 at 270°C.

TABLE 3

The Bulk Phase Composition of 10% Fe/Al_2O_3 during the 10% CO/H_2 Reaction and then H_2 Reduction at 270°C

Time (min)	Fe (%)	Fe^{2+} (%)	Fe_xC (%)	χ-$Fe_{2.5}C$ (%)	ε'-$Fe_{2.2}C$ (%)	Total carbide (%)	Gas on stream
0	74.1	25.9	0	0	0	0	↑
6	74.9	22.8	0	0	2.3	2.3	
22	20.5	17.5	15.1	14	32.8	62.0	10% CO/H_2
46	8.4	15.9	11.0	27.2	37.5	75.7	
77	1.8	15.9	7.8	32.7	41.7	82.2	
110	0.5	15.6	6.0	28.7	49.0	83.8	↓
128	2.5	16.9	15.8	35.9	28.8	80.5	↑
139	27.0	17.0	12.5	30.4	13.0	55.9	Switch to H_2
155	61.1	18.8	0	19.3	0.7	20.0	
175	79.5	20.0	0	0.5	0	0.5	↓

and dissolved C, and less by the transferal of surface carbon (surface carbide) into dissolved carbon.

To study further the effect of the reacting gas composition on carburization, we have done the experiments reported in Fig. 19. It is seen that as the hydrogen content of the gas containing 10% CO is increased at 270°C from 0 to 90%, the amount of carbide formed after 16 min on stream goes from negligible to an approximate plateau as soon as a little hydrogen is present. These results support the idea that carburization is inhibited by an oxidized surface. Only a small concentration of H_2 is required to reduce the O/H ratio on the surface to a low value.

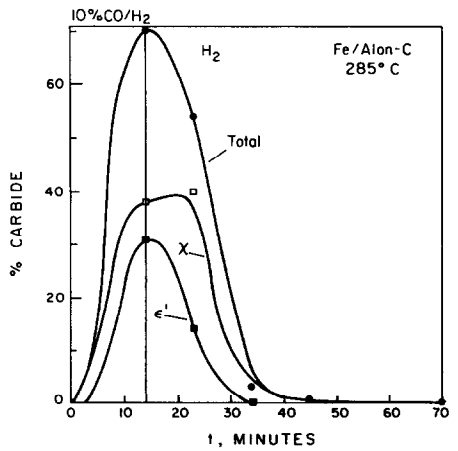

FIG. 15. Fe/Al_2O_3 (10%) carburized in 10% CO/H_2 and then decarburized in H_2 at 285°C.

Carbide Precursors

We recall that the results obtained by mass spectrometry (*1, 2*) show that after 16 min in 10% CO/H_2 at 270°C (or 285°C), an isothermal switch to hydrogen forms three peaks of methane. We have identified the first peak with surface CH, the second with surface carbide, and the third with bulk carbide (*2*). An idea of the reactivity of these species can be obtained by a switch to He rather than H_2 after 16 min. Then after various times in He (16 min more, for example), a final switch to H_2 shows the new shapes of the methane peaks formed. The basic result of this experiment (*2*) is that the exposure to helium does not change the CH peak, decreases the surface carbide peak, and increases the bulk carbide peak by an approximately equivalent amount. In the present work in Fig. 20 we show the MES results obtained during this experiment. After treatment in 10% CO/H_2 at 270°C for 16 min, the composition shown in A of Fig. 20 is obtained. Treatment in helium alone

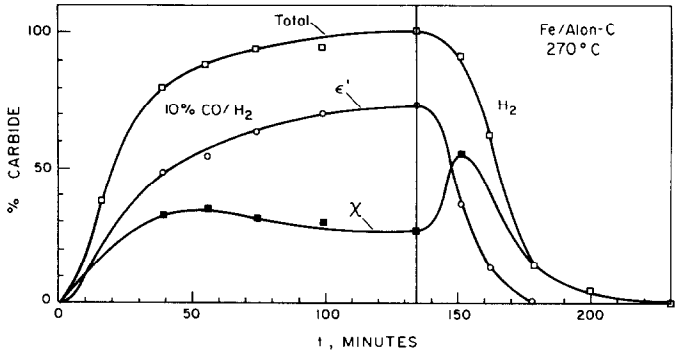

FIG. 16. Fe/Al_2O_3 (10%) carburized in 33% CO/H_2 and decarburized in H_2 at 270°C.

leads to more carburization (B), and heating further in helium leads to further carburization and a conversion from ε'- to χ-carbide, as expected at the higher temperature, 400°C. As already mentioned, 16 min in 10% CO/He leads to negligible carburization but considerable surface carbon buildup (E). A switch to 10% CO/H_2 now leads to a greater degree of carburization (F) than that shown in A or D. Some of the surface carbon formed by CO/He has added to that formed by the subsequent CO/H_2 treatment.

It is interesting that the surface carbide leads to bulk carbide whereas the surface CH does not. We have exposed the reduced catalyst to 10% C_2H_4/H_2, which leads to lots of C_2H_6 and some C_1, C_3, and C_4 products (*2*). During 16 min of this treatment, no bulk carbide formation is observed by MES, as is to be expected, for the surface CH_x species probably correspond to $x \geq 1$.

Restructuring of synthesis catalysts. We have observed that the rate of carburization in 10% CO/H_2 is slower on a catalyst reduced at 460°C than on the same catalyst used for the CO/H_2 reaction at 270 or 285°C and then reduced in H_2 at these temperatures. This probably occurs because during the course of the synthesis, the crystallites are transformed from α-Fe (*bcc* structure) to χ- and ε'-carbides (*hcp* structures). The surface of the catalyst is also modified. The reduction at 460°C largely restores the orig-

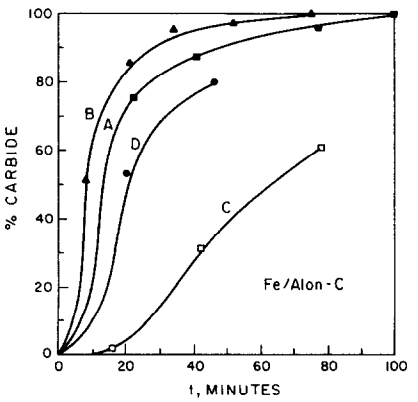

FIG. 17. Carburization of 10% Fe/Alon-C reduced 1 h at 460°C. (A) 10% CO/H_2 at 270°C; (B) 33% CO/H_2 at 270°C; (C) 10% CO/He at 270°C; (D) 10% CO/H_2 saturated with H_2O at 15°C, at 285°C.

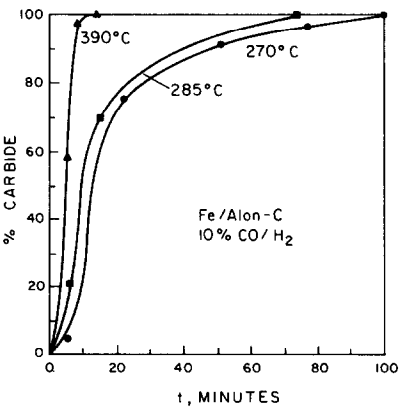

FIG. 18. Carburization of 10% Fe/Al_2O_3 by 10% CO/H_2 at different temperatures.

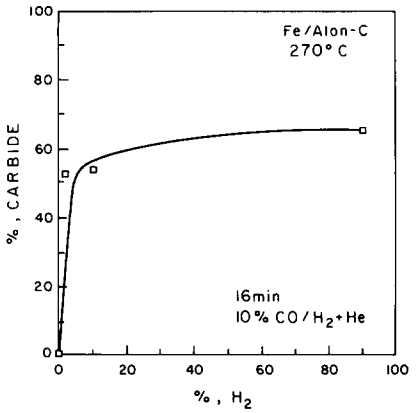

FIG. 19. Carburization of 10% Fe/Al_2O_3 at 270°C for 16 min with 10% CO and different concentrations of H_2; balance He.

inal structure, whereas that at 270 or 285°C does not. The extent to which this history of the catalyst influences the carburization and the extent to which the original structure of the catalyst can be restored (by decarburization with H_2) can be observed from the curves of Fig. 21.

It is proposed that a restructuring is caused by carburization, which if undisturbed by high-temperature reduction, maintains a solid more highly receptive to carburization. Thus carburization rates for a restructured solid are faster than those for a freshly reduced catalyst. The relative ratios of ε'- to χ-carbide remain the same for all curves. X-Ray diffraction studies on the appropriate samples showed no evidence of a change in particle size of the iron.

Fe/Cab-O-Sil 10%

The impregnated and dried catalyst exhibits the Mössbauer spectrum of Fe $(NO_3)_3$. A reduction sequence identical to the one used for the 10% Fe/Alon-C catalyst resulted in a Mössbauer spectrum indicating Fe^0 (85%) and Fe^{2+} (15%) species. The spectral parameters for the catalyst after treatment are shown in Table 4. The response of the T.C. detector and the transient response studies (*1, 2*) indicate a behavior similar to the alumina catalyst, but the activity per gram of the silica catalyst is about one-half. Studies on carburization and decarburization, identical to those for the alumina-supported catalyst, were conducted mainly at 285°C. The most significant differences were the lack of excessive surface carbon, and the low rate of carbide formation, both of which indicate a less active catalyst. The ratio of ε'- to χ-carbide was found to be higher in this catalyst.

Effect of CO, H_2, and H_2O. The effect of gas-phase concentrations is evident in the

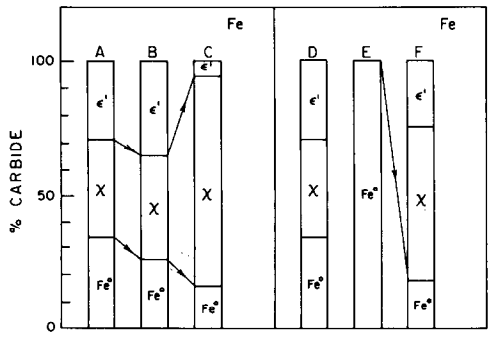

FIG. 20. Incorporation of surface carbon into the bulk of 10% Fe/Al_2O_3. (A) 16 min in 10% CO/H_2 at 270°C; (B) 16 min more in He at 306°C; (C) 16 min more in He at 400°C; (D) Same as (A); (E) 16 min in 10% CO/He at 270°C; (F) 16 min more in 10% CO/H_2 at 270°C.

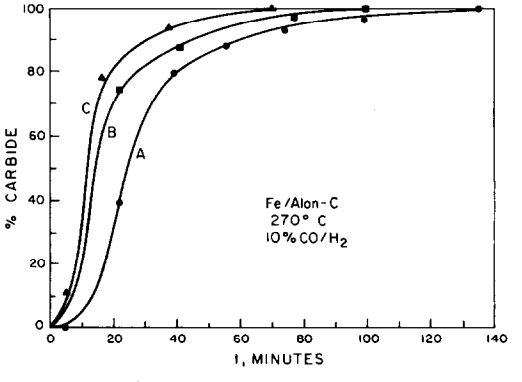

FIG. 21. Degree of carburization of 10% Fe/Alon-C in 10% CO/H_2 at 270°C. (A) Reduced catalyst of Fig. 2B; (B) Previously carburized catalyst decarburized in H_2 at 270°C and reduced at 460°C for 1 h; (C) Previously carburized catalyst decarburized by H_2 at 270°C only.

TABLE 4

Mössbauer Parameters of Fe Species Detected over 10% Fe/Cab-O-Sil at 297 K. Isomer Shift Values Reported with Respect to an α-Fe Standard

Catalyst treatment	Species	Spectral contribution (Area %)	Isomer shift, δ (mm/s)	Quadrupole splitting, ΔE_Q (mm/s)	Hyperfine field, H (kOe)
Catalyst as prepared and oven-dried	Fe^{3+}	100	0.33	0.72	0.0
Catalyst after the reduction sequence	Fe^0	85.5	0	0	330.0
	Fe^{2+} (a)		0.94	1.11	0.0
		14.5			
	Fe^{2+} (b)		1.01	1.80	0.0
Fully carburized catalyst after 10% CO/H_2 treatment	χ-Fe_5C_2 (I)		0.30		185
	(II)	11.1	0.38		218
	(III)		0.33		108
	ε'-$Fe_{2.2}C$	74.4	0.26		174
	Fe^{2+} (a)		0.96	1.20	0.0
		14.5			
	Fe^{2+} (b)		1.01	1.86	0.0

graphs of Fig. 22. Figures 22D and E represent the carburization rate in 10% CO/H_2 and 33% CO/H_2 at 250°C. As observed with the alumina-supported catalyst, an increase in the CO concentration increases the carburization rate. Moreover, Fig. 22A represents the rate of carburization with both 10% CO/H_2 and 33% CO/H_2 at 285°C. The curves are identical, indicating that the rate-limiting step in the carburization process does not involve the rate of surface carbon accumulation.

Comparison of Figs. 22D (base case), B (with no H_2), and C (with H_2O) indicate the strong influence of H_2 in promoting carburization and of H_2O in inhibiting it. As for the Alon-C catalyst, H_2 plays a key role in facilitating carburization. It is also important to note that carburization in the absence of H_2 is very slow in the silica-supported catalyst. The influence of H_2O is to delay carburization, and the effect is much stronger than for the alumina catalyst.

It is important to note in the carburization experiments that the rate of carburization is slower for the silica-based catalyst than for the alumina-based catalyst, even though the iron surface area of the silica catalyst is larger.

Studies with decarburization. There are differences in the decarburization of alumina- and silica-supported catalysts, as seen by Figs. 23 and 24. The decarburization is a more rapid process because of a lack of surface carbon permitting the decarburization of the carbide to start immediately.

If the carburization yields a mixture of ε'-

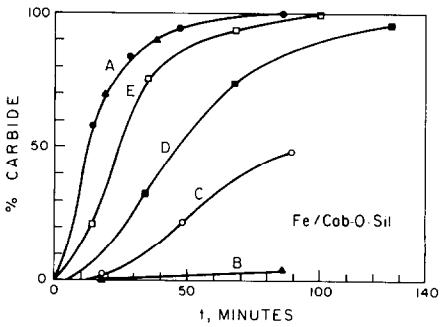

FIG. 22. Carburization of 10% Fe/SiO_2. (A) 10% CO/H_2 and also 33% CO/H_2 at 285°C; (B) 10% CO/He at 285°C; (C) 10% $CO/H_2 + H_2O$ at 285°C; (D) 10% CO/H_2 at 250°C; (E) 33% CO/H_2 at 250°C.

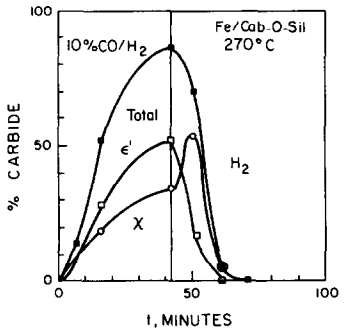

FIG. 23. Carburization of 10% Fe/SiO_2 at 270°C by 10% CO/H_2 and decarburization by H_2 at 270°C.

and χ-carbides, the decarburization exhibits a carbide transformation of e′ to χ prior to reduction to Fe^0. The rate-limiting step in the decarburization appears to be the interaction of the H_2 with the carbide/carbon on the surface, and the diffusion of the carbon in the crystallite is extremely rapid. As seen earlier, decarburization does not depend to a major extent on temperature, and reductions at 270–285°C yield the same rates of decarburization.

DISCUSSION

Evolution of the Carbides at 270°C

It has not previously been reported that iron crystallites supported on Al_2O_3 follow the progression $Fe^0 \rightarrow Fe_xC \rightarrow$ -$Fe_{2.5}C \rightarrow$ ε'-$Fe_{2.2}C$ at 270–285°C during carburization. Whether or not this sequence is followed depends on the environment of the iron, the temperature, and the gas composition. For unsupported iron (ex Fe_2O_3) this sequence was not observed (*5*), and for a catalyst similar to ours it was also not reported (*16*). Therefore, care must be exercised to interpret the MES results. For example, some doubt has been expressed about the existence of Fe_xC, and the stoichiometry of the ε'-form has been questioned (*18*). We prefer not to enter this debate and have followed the scheme used by Niemantsverdriet (*4*), supported by other studies (*10, 22*). By describing our spectra fully via Tables 1–4 we hope that our data will remain useful even if the nomenclature of the carbides changes.

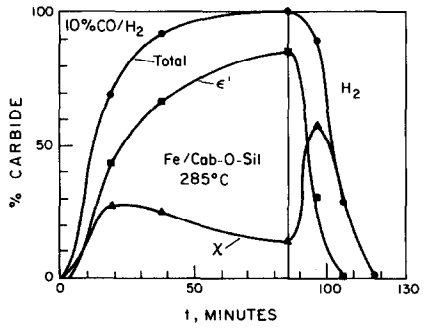

FIG. 24. Carburization of 10% Fe/SiO_2 at 285°C by 10% CO/H_2 and decarburization by H_2 at 285°C.

In support of the assumed carbon contents of the various carbides, we refer to our mass spectroscopy work (*1, 2*). The quantities of carbon corresponding to the carbide mixture observed agree with the nomenclature used. Note that Fig. 20 shows that the ε'-form converts to the χ-form as the temperature is raised above 300°C.

The computer work necessary to fit 40 peaks is quite burdensome. Starting values of the peak position, widths, and intensities close to the best value must be chosen manually with the program used (*20*), or the procedure will not converge. By extensive trials we have become convinced that a carbide Fe_xC ($x > 2.5$) must be included in order to represent the experimental spectra.

It is clear from the principles of MES that it would be desirable to record the spectra at 4 K rather than a 300 K as we have done. We are not equipped to operate at temperatures below ambient. Amelse *et al.* (*14*) have shown that the proportion of ε'- and χ-carbides apparent are a function of the observation temperature, and the lowest temperature should give the most reliable results. Thus the particular proportions of ε'- and χ-carbides we report may need to be adjusted when spectra taken at 4 K become available. Such work should be done *in situ*

in a cell capable of use both at 700–800 and 4 K (*6*). Studies at 4 K have shown the extreme sensitivity of iron catalysts to oxidation (*6, 14*). At any rate, it is probable that the evolution of carbide compositions which we have observed for isothermal carburization at 270–285°C will not be invalidated by measurements at 4 K, even though the ratio of the carbides at any moment may be changed.

Amelse *et al.* (*14*) have found that exposure of reduced iron to CO/H_2 at reaction temperature leads to the detection of increased oxide phases, when measurements are made at 4 K. In our room-temperature measurements, we do not see these oxides, so that the results shown in the first two rows of Table 3 are obtained, based on spectral areas. The Fe^0 does not really go up after 6 min in H_2/CO; rather, some undetected oxides are formed, which are not taken into account in the observed Fe^0/Fe^{2+} ratio. The reverse effect is also seen in the last two rows of Table 3. The Fe^0 proportion should be less, and there persist some difficult-to-reduce oxides (*6*).

The results on decarburization via hydrogen are quite clear. The ε'-carbide goes right down, and the χ-carbide definitely goes through a maximum, as does the Fe_xC. These results are consistent with a passage $\varepsilon' \rightarrow \chi \rightarrow Fe_xC \rightarrow Fe^0$ during decarburization. Figures 10–13 show this sequence and leaves little room for another interpretation. Although it is probable the carburization follows the reverse evolution, we have no data on short times. It is not clear whether χ is really formed before ε', but it does seem plausible. The positions of the curves in Figs. 14–16 and 23–24 at times before the first data point are estimated by eye only.

Steps in the carburization process. In trying to explain the kinetics of carburization reference is often made to diffusion limitations. Although these effects may control rates for macroscopic particles (1 mm), such is not likely to be the case for particles of a size such as 200 Å. The penetration of a diffusing substance into an infinite medium is given by

$$\delta = 4\sqrt{D_{AB}t}$$

where D_{AB} is the diffusion coefficient and t is the time. For carbon in α-iron at 250°C, Wert (*23*) gives a value of 10^{-10} cm^2/s, independently obtained by several investigators using various methods. This value means that to obtain a penetration depth of 100 Å, only about 6×10^{-4} s are required. Diffusion limitations are therefore unlikely.

In addition, in diffusion-controlled carburization, the carburized region should advance as a front, and the proportions of the various carbides should not change with time.

As a matter of fact, the sensitivity of the rate of carburization to gas composition, and thus surface composition, shown by Figs. 17 and 19, argues that the rate-controlling process at about 270°C must be associated with the surface. This matter has been discussed in our previous work (*2*) in which we propose that an active carbon, present in low concentration, is the precursor of the observed surface and bulk species. In particular, surface carbide can form bulk carbide by reacting back through the active carbon. This scheme explains the sensitivity of the carburization rate to the surface composition, in particular the O/H ratio as effected by the presence of H_2 or H_2O in the reacting gas.

The MES results of the present paper support those of our previous transient studies via mass spectrometry (*1, 2*) and give us some added insight into some details of the processes involved.

The silica-supported iron is definitely less reactive for carburization than the alumina-supported iron. However, there were not sufficient qualitative differences observed between the two catalysts to give any basis for an explanation of the observed support effects.

ACKNOWLEDGMENT

We are grateful to the National Science Foundation for support under Grant ENG 7821890. We also appreciate the helpful comments of W. N. Delgass.

REFERENCES

1. Bianchi, D., Borcar, S., Teule-Gay, F., and Bennett, C. O., *J. Catal.* **82,** 442 (1983).
2. Bianchi, D., Tau, L. M., Borcar, S., and Bennett, C. O., *J. Catal.* **84,** 352 (1983).
3. Vannice, M. A., *J. Catal.* **37,** 449 (1975).
4. Niemantsverdriet, J. W., thesis, Delft, 1983.
5. Niemantsverdriet, J. W., van der Kraan, A. M., van Dijk, W. L., and van der Baan, H. S., *J. Phys. Chem.* **84,** 3363 (1980).
6. Niemantsverdriet, J. W., Flipse, C. F. J., van der Kraan, A. M., and van Loef, J. J., *Appl. Surf. Sci.* **10,** 302 (1982).
7. Raupp, G. B., and Delgass, W. N., *J. Catal.* **58,** 337 (1979).
8. Raupp, G. B., and Delgass, W. N., *J. Catal.* **58,** 348 (1979).
9. Raupp, G. B., and Delgass, W. N., *J. Catal.* **58,** 361 (1979).
10. Amelse, J. A., Butt, J. B., and Schwartz, L. H., *J. Phys. Chem.* **82,** 558 (1978).
11. Unmuth, E. E., Schwartz, L. H., and Butt, J. B., *J. Catal.* **61,** 242 (1980).
12. Unmuth, E. E., Schwartz, L. H., and Butt, J. B., *J. Catal.* **63,** 404 (1980).
13. Amelse, J. A., Schwartz, L. H., and Butt, J. B., *J. Catal.* **72,** 95 (1981).
14. Amelse, J. A., Grynkewich, G., Butt, J. B., and Schwartz, L. H., *J. Phys. Chem.* **85,** 2484 (1981).
15. Jung, H-J, Vannice, M. A., Mulay, L. N., Stanfield, R. M., and Delgass, W. N., *J. Catal.* **76,** 208 (1982).
16. Nahon, Nicole, thesis, Lyon, 1979.
17. Delgass, W. N., and Chen, Ling-Yuan, *Rev. Sci. Instrum.* **47**(8), 968 (1976).
18. Le Caer, G., Dubois, J. M., Pijolat, M., Perrichon, V., and Brussiere, P., *J. Phys. Chem.* **86,** 4799 (1982).
19. Nagakura, S., Oketani, S., *Trans. Iron Steel Inst. Jpn.* **8,** 265 (1968).
20. Chrisman, B. L., and Tumolillo, T. A., *Comp. Phys. Commun.* **2,** 322 (1971).
21. Wilson, W., and Swartzendruber, L. J., *Comp. Phys. Commun.* **7,** 151 (1975).
22. Le Caer, G., Dubois, J. M., and Senateur, J. P., *J. Solid State Chem.* **19,** (1976).
23. Wert, C. A., *Phys. Rev.* **79,** 601 (1950).